Attosecond control of dissociative ionization of O_2 molecules

W. Siu,[1] F. Kelkensberg,[1] G. Gademann,[1] A. Rouzée,[1,2] P. Johnsson,[1,3] D. Dowek,[4] M. Lucchini,[5] F. Calegari,[5] U. De Giovannini,[6] A. Rubio,[6] R. R. Lucchese,[7] H. Kono,[8] F. Lépine,[9] and M. J. J. Vrakking[1,2]

[1]*FOM Institute AMOLF, Science Park 104, NL-1098 XG Amsterdam, The Netherlands*

[2]*Max-Born-Institut, Max-Born Strasse 2A, D-12489 Berlin, Germany*

[3]*Department of Physics, Lund University, Post Office Box 118, SE-221 00 Lund, Sweden*

[4]*Laboratoire des Collisions Atomiques et Moléculaires (UMR Université Paris-Sud et CNRS, 8625), Bâtiment 351, Université Paris-Sud, F-91405 Orsay Cedex, France*

[5]*Department of Physics, Politecnico di Milano, Istituto di Fotonica e Nanotecnologie CNR-IFN, Piazza Leonardo da Vinci 32, 20133 Milano, Italy*

[6]*Nano-bio Spectroscopy Group, ETSF Scientific Development Centre, Universidad del País Vasco, Avenida Tolosa 72, E-20018 San Sebastián, Spain*

[7]*Department of Chemistry, Texas A&M University, Post Office Box 30012, College Station, Texas 77842-3012, USA*

[8]*Department of Chemistry, Graduate School of Science, Tohoku University, Sendai 980-8578, Japan*

[9]*Université Lyon 1/CNRS/LASIM, UMR 5579, 43 Boulevard Du 11 Novembre 1918, F-69622 Villeurbane, France*

(Received 6 June 2011; published 14 December 2011)

We demonstrate that dissociative ionization of O_2 can be controlled by the relative delay between an attosecond pulse train (APT) and a copropagating infrared (IR) field. Our experiments reveal a dependence of both the branching ratios between a range of electronic states and the fragment angular distributions on the extreme ultraviolet (XUV) to IR time delay. The observations go beyond adiabatic propagation of dissociative wave packets on IR-induced quasistatic potential energy curves and are understood in terms of an IR-induced coupling between electronic states in the molecular ion.

DOI: 10.1103/PhysRevA.84.063412 PACS number(s): 33.20.Xx, 32.80.Qk

I. INTRODUCTION

The electronic response of matter to incident light in the visible to ultraviolet (UV) wavelength region occurs on the attosecond time scale [1]. The resulting electronic excitation processes can lead to ultrafast charge rearrangement and migration processes and has been predicted in midsize molecules of chemical and biological interest following the removal of an electron on attosecond time scales [2,3]. A crucial task ahead is the experimental validation of these predictions by probing the electron dynamics in molecules in real time. So far all available evidence for ultrafast charge migration processes has been indirect. For example, charge migration has been implicated in experiments where peptide ions dissociated in a bond-selective manner after ionization [4], as well as in high-order-harmonic generation (HHG) experiments where the measured extreme ultraviolet (XUV) spectrum revealed sub-femtosecond hole dynamics [5].

In the past decade, experimental techniques have been developed that allow one to address rapid electron dynamics on (sub-)femtosecond time scales. Pump-probe spectroscopy using attosecond light pulses generated by HHG [6] has been developed and applied in pioneering experiments on atoms, molecules, and condensed matter [7–10].

In the context of these developments, it becomes of crucial importance to address the question how, in an attosecond or few-femtosecond time-resolved experiment, electron dynamics can be revealed and controlled in molecules. Previously we have reported on measurements of laboratory frame fragment asymmetries (i.e., an imbalance between the number of fragment ions that fly upward or downward along the laser polarization axis) that arises in dissociative ionization of D_2 using carrier-envelope-phase-stabilized few-cycle laser pulses [11] and in a two-color XUV + infrared (IR) pump-probe experiment on H_2 and D_2 Ref. [8]. The observation of an asymmetric fragment ejection signifies the occurrence of electron localization. The observed dependence of the asymmetry in Ref. [8] on the relative timing of the two pulses signifies an attosecond-time-scale electronic response of the molecule under investigation. However, such measurements do not yet allow one to track and control the electronic motion that leads to the observable electron localization. To this end, experiments need to be developed where attosecond laser pulses probe the ultrafast electron dynamics rather than initiating it. Recently, we have taken first steps toward this goal in experiments where we used attosecond pulses to probe electron dynamics in H_2 and D_2 molecules [12]. The yield and angular distribution of $H^+(D^+)$ fragment ions were seen to depend on the XUV-IR delay. Given the simplicity of the electronic states of hydrogen and its molecular ion, these experiments could be interpreted in terms of two-color interferences involving two ionization continua. The conclusion was that the photoionization was favored under conditions where the IR field induced a localization of the electron in the ion. It remains an open question to what extent electron dynamics can be probed or controlled on the attosecond time scale in larger molecules, where the initial response of the molecule may be inherently multielectron in nature. As a first step toward addressing this question, we report on experiments where dissociative ionization of O_2 is controlled by means of the relative time delay between an attosecond pulse train (APT) and a copropagating IR field. We present experimental measurements of ionic fragmentation patterns that show that, using the relative XUV-IR delay as a control knob, we can control the electron dynamics in the molecule and thereby the branching ratio of different ionic fragmentation channels.

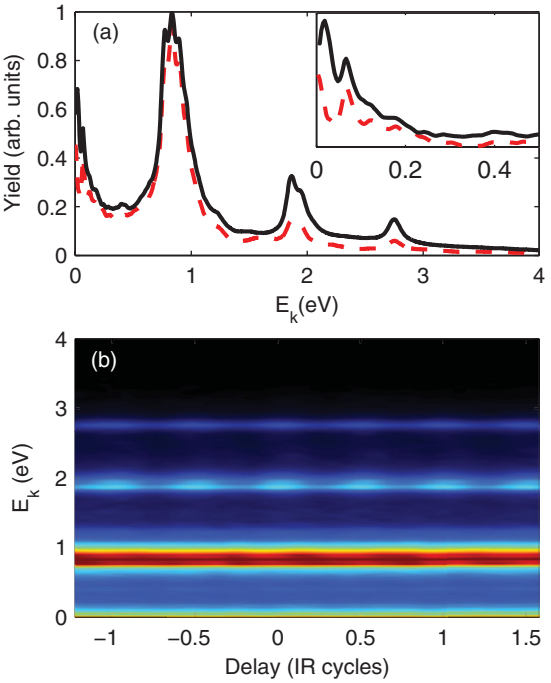

FIG. 1. (Color online) (a) O^+ kinetic energy spectrum, resulting from XUV-only ionization (red dashed line), along with the kinetic energy spectrum for XUV + IR ionization, averaged over one full period of the XUV + IR delay (solid black line). The kinetic energy spectrum for $E_k < 0.5$ eV is plotted in the inset and shows various sharp features on top of a broad contribution. (b) Dependence of the angle-integrated kinetic energy spectrum on the time delay between the XUV and IR pulses.

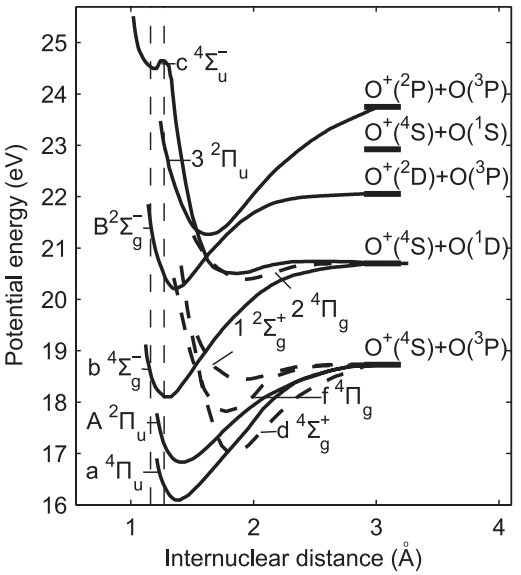

FIG. 2. Potential energy curves for the O_2^+ molecular states. The energy scale refers to the O_2 ground state, and the Franck-Condon region is indicated by vertical dashed lines. Data taken from Refs. [14,15].

II. EXPERIMENTAL METHOD

In the experiment, 30-fs full width at half-maximum (FWHM) IR pulses (linear polarization, $\lambda = 780$ nm) were equally split into two beams. One beam was used to generate an XUV APT by HHG in Xe. The IR field and lower-order harmonics were filtered out using a 200-nm aluminium filter. The resulting XUV spectrum consisted of harmonics 11–21 of the driving laser frequency (17.5–33.4 eV). The XUV and IR beams were colinearly focused into a velocity map imaging spectrometer, where O_2 molecules were introduced by a pulsed valve that was integrated into the repeller electrode [13]. The three-dimensional momentum distribution of O^+ fragments, resulting from the (two-color) dissociative ionization, was measured. The IR intensity of approximately 5×10^{12} W/cm^2 was too low to produce any ionic fragments by itself.

III. RESULTS

The angle-integrated kinetic energy spectrum of O^+ fragments, resulting from ionization with only the XUV pulse, is shown in Fig. 1(a) (red dashed line).

The photoion spectrum in Fig. 1(a) contains four main contributions around E_k = 0–0.2, 0.9, 1.9, and 2.9 eV. The contribution at $E_k = 0.9$ eV is dominantly assigned to dissociative photoionization (DPI) following formation of the $B\ ^2\Sigma_g^-$ (v = 0–3) ion state (see Fig. 2) and dissociation to the first dissociation limit $[O^+(^4S) + O(^3P)]$ [14,15]. The contributions at $E_k = 1.9$ and 2.9 eV are assigned to DPI following formation of the $c\ ^4\Sigma_u^-$ (v = 0,1) ion state and dissociation to respectively the second $[O^+(^4S) + O(^1D)]$ and first dissociation limits [14,15]. In the lower-energy region of E_k = 0–0.2 eV (see inset), sharp features are observed that are due to DPI involving excitation of the O_2^* $(3\ ^2\Pi_u, ns\sigma_g)$ autoionizing state and dissociation to the third $[O^+(^2D) + O(^3P)]$ dissociation limit [14,16], as well as formation of the $b\ ^4\Sigma_g^-$ and $B\ ^2\Sigma_g^-$ of the molecular ion, followed by dissociation to respectively the first and second dissociation limits [14]. In addition, dissociation following the formation of the $3\ ^2\Pi_u$ state contributes significantly to the formation of fragment ions with $E_k \sim$ 0–1 eV [14]. Minor contributions to the fragment ion kinetic energy spectrum may be due to additional DPI pathways involving higher lying ionic states and/or the excitation of excited neutral states followed by dissociation and autoionization [17].

When the ionization by the APT takes place in the presence of an IR field, significant changes are observed in the kinetic energy spectrum. The O^+ kinetic energy spectrum for XUV + IR ionization, resulting from averaging over a range of delays spanning a full cycle of the IR field, is shown in Fig. 1(a) (solid black line) and shows an increase in the fragment ion yield over a large range of kinetic energies. This increase is particularly pronounced for the contributions centered at $E_k = 1.9$ and 2.9 eV (related to formation of the $c\ ^4\Sigma_u^-$ state).

The enhancement depends with attosecond time resolution on the relative XUV-IR delay. This is shown in Fig. 1(b), where the angle-integrated kinetic energy spectra are plotted as a function of the XUV-IR delay. The delay dependence of the angle-integrated yields of the fragment ion channels involving the $B\ ^2\Sigma_g^-$ ($E_k = 0.9$ eV) and $c\ ^4\Sigma_u^-$ ($E_k = 1.9$ and 2.9 eV) ionic states are shown in Figs. 3(a)–3(c). In addition, an energy

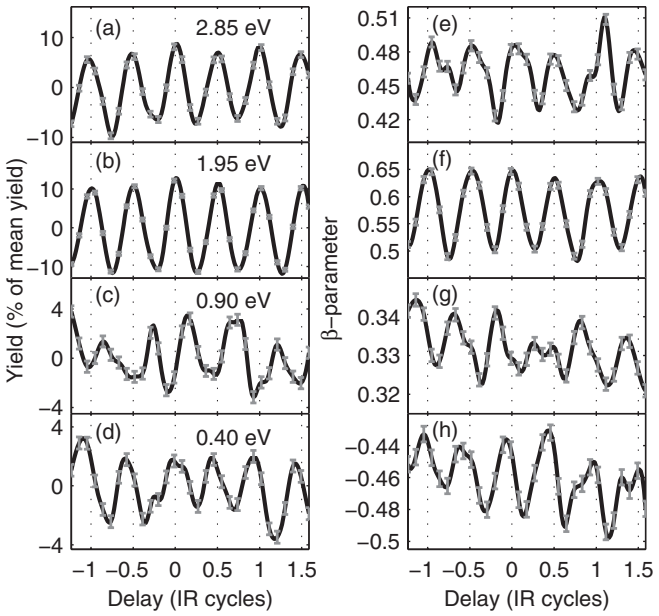

FIG. 3. The fragment yield oscillations for the individual channels, resulting from an energy integration ($\Delta E = 0.2$ eV) of Fig. 1(b) are shown for E_k = (a) 2.9 eV, (b) 1.9 eV, (c) 0.9 eV, and (d) 0.4 eV. The accompanying delay dependence of the $\beta(E_k,t)$, describing the fragment ion angular distribution is shown in panels (e)–(h). In the experiment, it is found that the period of half the IR cycle did not exactly match the periodicity of the yield oscillations, due to thermal drifts in the interferometer. The delay axis is adjusted to accommodate two yield oscillations within one optical cycle of the IR field (λ = 750 nm). The dotted lines are spaced by a half period of the IR cycle and coincide with the maxima in the fragment ion yield in the E_k = 1.9 and 2.9 eV channels.

integration around $E_k = 0.4$ eV is shown in Fig. 3(d), which involves the $3\,^2\Pi_u$ state. An energy integration in the E_k = 0.1 eV region showed a yield oscillation with a modulation depth of only $\pm 1.5\%$ and is therefore not included in the following discussion.

In all of the chosen DPI channels, the oscillations in the fragment ion yields have a period that is half the period of the IR cycle, indicating a dependence on the magnitude of the IR electric field at the time of ionization. Since the experiment is performed with an APT that contains two attosecond pulses per optical cycle, a possible dependence on the sign of the laser electric field cannot be revealed in these measurements since consecutive pulses in the train sample IR half-cycles with the opposite sign of the electric field. Interestingly, the fragment ion yield for XUV + IR ionization is always higher than for XUV-only ionization at all delays. The observed attosecond time dependence may have a number of different origins. On the one hand, the observed dependence may arise as a result of a purely electronic response involving electronic motion in neutral or ionic molecular states (or both), or, on the other hand, it may involve the coupling of the electronic and nuclear degrees of freedom during the fragmentation process.

A useful point of departure is to consider whether the observations fit within a quasistatic picture, that is, a description of the XUV ionization process in the presence of a quasistatic IR-induced electric field, in combination with an adiabatic dissociation of the molecular ion states. In this view, one would expect that the photoion kinetic energy spectrum, measured at delays where the attosecond pulses are synchronized to the zero-crossings of the IR field, is similar to the photoion spectrum for single-color ionization by the XUV pulse. The well-synchronized oscillations for the 2.85- and 1.95-eV channel in Figs. 3(a) and 3(b), which have a common origin in the formation of the $c\,^4\Sigma_u^-$ state, suggests the possibility of such a quasistatic, purely electronic, IR-mediated population of the $c\,^4\Sigma_u^-$ state, without the involvement of nuclear dynamics. When considering the quasistatic picture, one may question whether the dominant electronic couplings occur in the neutral or ionic system. By analogy with the existing literature on Rydberg wave packets [18], we expect that the occurrence of IR-induced admixtures of electronic states in the neutral molecule might affect the total O^+ and O_2^+ ion yield. At the same time, we expect that IR-induced couplings between the ionic states may lead to time-dependent variations in the ion yield from specific fragmentation channels. In the present experiment, measurements of the O_2^+ yield showed no delay dependence in excess of the existing experimental uncertainty of 1–2%. The experimental data therefore might suggest that the couplings in the molecular ion are more important. This conclusion is similar to the one reached in the earlier case of H_2 [12].

However, the experiment also contains important observations that lead us to question the validity of a quasistatic description. The amplitude of the IR-induced oscillations is much smaller than the overall IR-induced enhancement of the fragment ion yield. Furthermore, the yield oscillations that we observe for the different ionic states in Figs. 3(a)–3(d) are not exactly all in or out of phase. This suggests that additional dissociation pathways that are induced by the IR field, involving sequential excitations, may play an important role. Such sequential dissociative ionization pathways may also display a subcycle delay dependence, as was revealed, for example, by fragment kinetic energy spectra measured for the Coulomb explosion of H_2 [19].

When a quasistatic description does not suffice, a dynamical description of the dissociative ionization process becomes necessary. An exact theoretical model, which needs to include both the coupled electronic and nuclear motion, is not solvable analytically, and one has to resort to numerical techniques. We hope that using methods such as time-dependent density functional theory (TDDFT), multiconfiguration time-dependent Hartree-Fock (MC-TDHF), or multiconfiguration self-consistent field (MC-SCF) such results may soon be forthcoming.

In addition to the ion yield oscillations, IR-induced effects are also experimentally observed in the O^+ angular distributions. The fragment ion angular distribution is well described by $P[E,\cos(\theta),t] \sim 1 + \beta(E,t)P_2[\cos(\theta)]$, as higher order terms in $P[E,\cos(\theta)]$ are found to be negligible. The β parameters for the previously selected DPI channels are plotted as a function of delay in Figs. 3(e)–3(h). Oscillations in the β parameter are observed for all the selected channels with a period of half the IR period. The β parameters for XUV-only ionization are comparable to the values found in Ref. [20]. We observe an increase in the β parameters of 0.6

and 0.3 for the $E_k = 1.95$ and 2.85 eV channels ($c\,^4\Sigma_u^-$ state), respectively. In addition to control over the fragment ion yield, we therefore observe that the fragment angular distribution can be controlled by changing the XUV-IR delay.

The dependence of the fragment angular distribution on the XUV-IR delay can be understood by considering the fact that the XUV ionization occurs from a neutral (initial) state to a system in which molecular ion + continuum electron (final) states are coupled to each other by the IR field. The latter coupling is favored for molecules aligned along (perpendicular to) the laser polarization when the associated ionic transition is parallel (perpendicular). In other words, coupling among molecular ion states with the same symmetry is accompanied by a parallel transition and leads to a situation where an increase in the ion yield is accompanied by a sharpening of the angular distribution along the laser polarization and hence an increase of the β parameter. Conversely, the observation of an increase in the ion yield accompanied by a decrease of the β parameter signifies the involvement of a perpendicular transition. In formulating these relations, we considered that couplings between molecular ion + electron states in which the molecular ion and continuum electron both change in electronic character are less important than couplings in which only the molecular ion changes in electronic state.

In the experimental results, we observe that the fragment yield and β-parameter oscillations are in phase for the contributions related to the $c\,^4\Sigma_u^-$ state ($E_k = 1.9$ and 2.9 eV). Considering also the role of spin selection rules [21], we postulate that this observation can be explained by a coupling of the $c\,^4\Sigma_u^-$ state to the $b\,^4\Sigma_g^-$ state. A similar in-phase oscillation of the ion yield and β-parameter oscillations is also observed for the $3\,^2\Pi_u$ ($E_k = 0.4$ eV) state, and we consider a coupling of this state to the bound $X\,^2\Pi_g$ or $A\,^2\Pi_u$ states to be the most likely mechanism. Conversely, we observe that the fragment yield and β-parameter oscillations for the $B\,^2\Sigma_g^-$ ($E_k = 0.9$ eV) state appear to be out of phase, although a clear phase relation between the two cannot be determined. A perpendicular coupling of this state to the bound $X\,^2\Pi_g$ or $A\,^2\Pi_u$ states could explain the experimental observations.

IV. CONCLUSION

In conclusion, we have shown that dissociative ionization of O_2 molecules by a two-color XUV + IR laser field can be controlled by the relative time delay between the IR field and the APT. In the future, ion-electron coincidence measurements may be able to provide more complete knowledge about the molecular ion states that are involved in the coupling and shed more light on the physical mechanisms. Our results support the notion that an attosecond electron response of a system can be used to control the outcome of a chemical reaction.

ACKNOWLEDGMENTS

This work is part of the research program of the Stichting voor Fundamenteel Onderzoek der Materie (FOM), which is financially supported by the Nederlandse organisatie voor Wetenschappelijk Onderzoek (NWO). P.J. acknowledges support from the Swedish Research Council.

[1] J. Breidbach and L. S. Cederbaum, Phys. Rev. Lett. **94**, 033901 (2005).
[2] A. I. Kuleff and L. S. Cederbaum, Chem. Phys. **338**, 320 (2007).
[3] F. Remacle and R. D. Levine, Proc. Natl. Acad. Sci. USA **103**, 6793 (2006).
[4] R. Weinkauf *et al.*, J. Phys. Chem. **99**, 11255 (1995).
[5] S. Haessler *et al.*, Nat. Phys. **6**, 200 (2010).
[6] P. M. Paul *et al.*, Science **292**, 1689 (2001).
[7] M. Uiberacker *et al.*, Nature (London) **446**, 627 (2007).
[8] G. Sansone *et al.*, Nature (London) **465**, 763 (2010).
[9] A. L. Cavalieri *et al.*, Nature (London) **449**, 1029 (2007).
[10] S. Haessler *et al.*, Phys. Rev. A **80**, 011404 (2009).
[11] M. F. Kling *et al.*, Science **312**, 246 (2006).
[12] F. Kelkensberg *et al.*, Phys. Rev. Lett. **107**, 043002 (2011).
[13] O. Ghafur *et al.*, Rev. Sci. Instrum. **80**, 033110 (2009).
[14] A. Lafosse *et al.*, J. Chem. Phys. **114**, 6605 (2001).
[15] Y. Lu *et al.*, J. Electron Spectrosc. Relat. Phenom. **94**, 135 (1998).
[16] P. M. Guyon, A. V. Golovin, C. J. K. Quayle, M. Vervloet, and M. Richard-Viard, Phys. Rev. Lett. **76**, 600 (1996).
[17] P. Erman *et al.*, J. Phys. B **29**, 5785 (1996).
[18] J. Parker and C. R. Stroud, Phys. Rev. Lett. **56**, 716 (1986).
[19] A. Staudte *et al.*, Phys. Rev. Lett. **98**, 073003 (2007).
[20] A. Lafosse *et al.*, J. Chem. Phys. **117**, 8368 (2002).
[21] G. Herzberg, *Molecular Spectra and Molecular Structure*, 2nd ed., Vol. 1 (D. Van Nostrand, Ottawa, 1950).